ELSEVIER

Size- and Composition-Resolved Externally Mixed Aerosol Model

Lynn M. Russell and John H. Seinfeld*

DEPARTMENT OF CHEMICAL ENGINEERING, PRINCETON UNIVERSITY, PRINCETON, NJ, USA
DEPARTMENT OF CHEMICAL ENGIENEERING, CALIFORNIA INSTITUTE OF TECHNOLOGY, PASADENA, CA, USA

ABSTRACT. The need for a numerical algorithm to predict the growth of external mixtures of aerosol populations is common to several current areas of study, including aerosol radiative effects, particle production processes, and pollution source apportionment. This work describes a model that solves this problem for explicit external and internal mixtures for the processes of coagulation, condensation, deposition, activation, and nucleation. The solution is numerically accurate for both particulate mass and number conservation by virtue of a dual-moment sectional method for solute growth. In addition, evaporable components are calculated in moving sections to retain information during particle activation in supersaturated conditions. The model is illustrated by application to the problem of cloud processing in a marine boundary layer capped with a layer of stratus clouds. The aerosol population is tracked in an air parcel circulating within the boundary layer and through the cloud layer. Boundary layer structure and cloud supersaturation profiles are predicted from gradients of observed thermodynamic variables. The model shows the differential growth of particles during cloud processing in two different types of particle populations, one of sea-salt origin and the other of sulfate origin.
AEROSOL SCIENCE AND TECHNOLOGY 28:403–416 (1998)

INTRODUCTION

Most current models of atmospheric aerosol dynamics assume, largely for computational reasons, that atmospheric aerosols are an internal mixture. For many applications this is an adequate assumption, yet, for a number of situations, one desires to account explicitly for the fact that particles arise from different sources and tend to retain their "source identity" as they age in the atmosphere. This aim necessitates a treatment that accounts explicitly for the externally mixed nature of the aerosol—a problem in which accounting for the source identity of airborne particles is key to the effect of aerosols on climate. Although overall aerosol direct radiative forcing depends on the total mass of aerosol in the atmosphere, the way in which absorbing and scattering components of the particles are distributed can have a significant effect on radiative forcing (Haywood and Shine, 1995; Liao and Seinfeld, 1998). Another important issue that requires tracking multiple particle populations are the hygroscopic and cloud condensation nucleus properties of particles; it is

*Corresponding author.

Aerosol Science and Technology 28:403–416 (1998)

Published by Elsevier Science Inc.

0278-6826/98/$19.00
PII S0278-6826(97)00248-1

well established that atmospheric aerosol properties frequently have hygroscopic and nonhygroscopic components.

Determining the relative importance of different particle sources to the overall aerosol population requires the capability of differentiating among particle populations as they evolve simultaneously. Several studies have investigated the role of internal mixtures in vapor-particle equilibria and heterogeneous chemistry (Hegg, 1990; Wexler and Seinfeld, 1992; Kreidenweis et al., 1993; Pandis et al., 1994; Russell et al., 1994). Models used in these studies have assumed that particles are homogeneous for each size class. As noted above, differences among particle sources result in significant differences in composition for particles of the same size. By considering independent populations of particles one can investigate such issues as the nucleation of new particles in the presence of a seed aerosol population, and the impact of anthropogenic aerosol on cloud processes as compared with that of natural particles. The goal of this work is to present a general multicomponent, multipopulation aerosol model that includes all important phenomena for aerosol dynamics and aerosol-cloud interactions: condensation, coagulation, aerosol thermodynamics, cloud droplet activation, and removal processes.

We consider multiple, distinct aerosol populations in an externally mixed, fixed-sectional model that includes nucleation, condensation, coagulation, and deposition processes. Particle growth and evaporation under supersaturated conditions are calculated by explicit accounting of wet and dry particle size to differentiate the separate compositions of activated particles. The ability of different particle populations to serve as sites for cloud droplet activation provides the basis for estimating the impact of anthropogenic emissions on cloud properties. In this way one can investigate, for example, aerosol-cloud interactions from a number of marine boundary layer sources, including sea spray, biogenic sulfur, and ship stack combustion products. To track accurately the growth of particle number from one mode to a larger mode that results from condensational growth of an aerosol population requires a numerical algorithm accurate for both the zeroth (number) and third (mass) moments of the particle-size distribution.

Although the sectional method is accurate and efficient for evaluating coagulation kernels, it generally has been applied to simulate aerosol growth on a mass conservation basis, which may not necessarily conserve particle number. We introduce here both number and mass conservation properties into the numerical algorithm used to track aerosol growth and evaporation. Assessing the impact of supersaturated conditions on aerosol-size distributions requires consideration of aqueous chemical processing. For this reason, it is desirable to retain unactivated or solute particle-size information during calculations of cloud droplet evolution.

Ambient particle and droplet diameters and activities are calculated based on aqueous solutions of the dry particle solutes. Upon activation, size segregation of the dry solute masses is retained so that multiple unactivated particle-size categories are kept distinct from the less-resolved droplet size categories. By retaining these pre-activation categories the calculation of evaporation recovers the original size distribution, modified only by addition of condensates during cloud processing. To investigate how many nominal cloud condensation nuclei (CCN) activate at a particular cloud supersaturation requires modeling the condensation rate during updraft into cloud as supersaturation increases. In this way, maximum supersaturation, ultimate droplet size, and number of droplets formed are determined by the more accurate kinetic rather than equilibrium Köhler theory approach.

A case study based on aerosol and cloud measurements collected in the marine boundary layer near Monterey, CA, in June 1994 will be used to illustrate the application of the model. Marine stratus clouds form when moist air from the surface is supersaturated by cooling as it is lifted to the top of the boundary layer. The resulting growth of particles (of about 0.2 μm in diameter) to

cloud droplets (of more than 10 μm in diameter) changes the particle population in both its size and chemical constituency. To simulate the role of clouds in aerosol formation and growth processes, we study this system with the detailed numerical model here, which is capable of representing both clear air aerosol evolution and the microphysical changes engendered by cloud formation.

Previous modeling studies of aerosol/cloud interactions in the marine boundary layer each have had limitations in the degree to which complete size- and composition-resolved aerosol-cloud interactions can be represented, in part resulting from computational constraints. The comprehensive size- and chemically-resolved microphysical model of aerosol-cloud interactions presented here is able to address, for example, the following questions: (a) What is the relative importance of distinct particle source contributions, for example, wave-generated sea salt particles, marine sulfate sources, and anthropogenic emissions in serving as cloud condensation nuclei? (b) What is the relationship between the aerosol mass increase resulting from condensation, and how does this increase in mass control the shift of particle numbers from one mode to the next? (c) How rapidly do droplets activate in weakly supersaturated conditions, and is this process equilibrium-controlled or rate limited?

PROCESSES CONTROLLING AEROSOL EVOLUTION

The model structure is designed to be able to account for independent particle populations in an external mixture. This feature provides the ability to track particle nuclei through condensational and coagulational growth so that the source of particle number can be identified directly rather than from deductions based on particle mass. Since particle number is the property that determines many aerosol properties, such as cloud droplet concentration in the atmosphere, this model provides the ability to assess the role of aerosol sources in the indirect effect of cloud properties on radiation (National Research Council, 1996).

We will use M_p to denote particulate mass and N_p the number of particles. In keeping with a sectional description of the particle-size distribution, we use the subscript i to denote the index for the size of the section. To designate an external mixture of aerosols, the subscript k is the index for the population of aerosols. The index j is used to track each component j in an internal mixture in particles of population k at size i. The expression $N_{p_{ik}}$ then refers to the number of particles of population k in section i and $M_{p_{ijk}}$ refers to the particulate mass of component j in the aerosols of population k in section i.

Externally and Internally Mixed Aerosol Dynamics

The change in number concentration is governed by

$$\frac{\partial N_{p_{ik}}(t)}{\partial t} = \left(\frac{\partial N_{p_{ik}}(t)}{\partial t}\right)^{\text{nucl}} + \left(\frac{\partial N_{p_{ik}}(t)}{\partial t}\right)^{\text{flux}} + \left(\frac{\partial N_{p_{ik}}(t)}{\partial t}\right)^{\text{depn}} + \left(\frac{\partial N_{p_{ik}}(t)}{\partial t}\right)^{\text{grow}} + \left(\frac{\partial N_{p_{ik}}(t)}{\partial t}\right)^{\text{coag}} \quad (1)$$

These mechanisms are summarized in Fig. 1.

$$\frac{dN_{p_{ik}}}{dt} = J_{ik}^{\text{nucl}} + J_{ik}^{\text{flux}} - K_{ik}^{\text{depn}} N_{p_{ik}} + J_{ijk}^{\text{grow}} + \frac{1}{2} \sum_{i_1 \le i} \sum_{i_2 \le i} \sum_{k_1 \le k} K_{i_1 i_2}^{\text{coag}} N_{p_{i_1 k_1}} N_{p_{i_2 k}} - \sum_{i_1 \le i_{\max}} \sum_{k_1 \le k_{\max}} K_{i_1 i}^{\text{coag}} N_{p_{i_1 k_1}} N_{p_{ik}} \quad (2)$$

The equation governing the change in particle mass including condensational growth then is given by

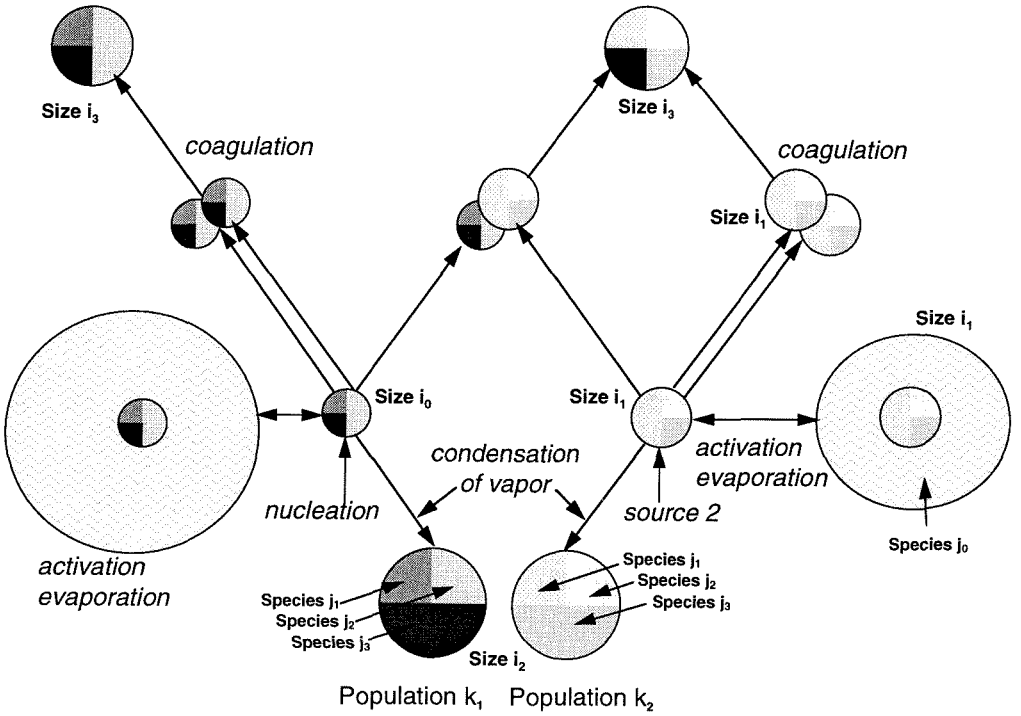

FIGURE 1. Diagram of mechanisms of particle dynamics described by the proposed algorithm.

$$\frac{\partial M_{\mathrm{p}_{ijk}}(t)}{\partial t} = \left(\frac{\partial M_{\mathrm{p}_{ijk}}(t)}{\partial t}\right)^{\mathrm{nucl}} + \left(\frac{\partial M_{\mathrm{p}_{ijk}}(t)}{\partial t}\right)^{\mathrm{flux}} + \left(\frac{\partial M_{\mathrm{p}_{ijk}}(t)}{\partial t}\right)^{\mathrm{depn}} + \left(\frac{\partial M_{\mathrm{p}_{ijk}}(t)}{\partial t}\right)^{\mathrm{cond}} + \left(\frac{\partial M_{\mathrm{p}_{ijk}}(t)}{\partial t}\right)^{\mathrm{coag}} \tag{3}$$

$$\begin{aligned}\frac{\partial M_{\mathrm{p}_{ijk}}(t)}{\partial t} = {} & \frac{M_{\mathrm{p}_{ijk}}}{\sum_j M_{\mathrm{p}_{ijk}}} m_{ik} J_{ik}^{\mathrm{nucl}} + \frac{M_{\mathrm{p}_{ijk}}}{\sum_j M_{\mathrm{p}_{ijk}}} m_{ik} J_{ik}^{\mathrm{flux}} - \frac{M_{\mathrm{p}_{ijk}}}{\sum_j M_{\mathrm{p}_{ijk}}} m_{ik} K_{ik}^{\mathrm{depn}} N_{\mathrm{p}_{ik}} \\ & + 2\pi \mathscr{D}_j D_{\mathrm{p}_{ik}}^{\mathrm{amb}} F(\mathrm{Kn}_{ik}) A(\mathrm{Kn}_{ik}) (P_j^{\infty} - P_{ijk}^{\mathrm{surf}}) \\ & + \frac{1}{2} \frac{M_{\mathrm{p}_{ijk}}}{\sum_j M_{\mathrm{p}_{ijk}}} m_{ik} \sum_{i_1 \le i} \sum_{i_2 \le i} \sum_{k_1 \le k} K_{i_1 i_2}^{\mathrm{coag}} N_{\mathrm{p}_{i_1 k_1}} N_{\mathrm{p}_{i_2 k}} \\ & - \frac{M_{\mathrm{p}_{ijk}}}{\sum_j M_{\mathrm{p}_{ijk}}} m_{ik} \sum_{i_1 \le i_{\max}} \sum_{k_1 \le k_{\max}} K_{i_1 i}^{\mathrm{coag}} N_{\mathrm{p}_{i_1 k_1}} N_{\mathrm{p}_{ik}}\end{aligned} \tag{4}$$

where m_{ik} is the mass of a single particle of population k in section i.

For each time step, both of these equations are numerically integrated. Similar to the approach adopted in the integral model of Warren and Seinfeld (1985a), both number and mass are accounted independently. By using two moments, the explicit changes

in mass and number are calculated separately, for both coagulation and condensation. In condensation, no new particles are added, but mass is added to preexisting particles. In coagulation, particles are lost from two sections, and gained by another section; the mass lost corresponds exactly to the number lost, but the mass gained may be a fraction of the number gained since the new particle may not correspond to an existing sectional diameter. The population identity of particles after coagulation and condensation is retained by an application-specific set of rules, designed to maintain the integrity of the population source. By using the volatility of particle components to provide a preference order, the characteristic involatile core, such as sea salt or elemental carbon, is retained with the particle population type to show the role of aged emissions in activation to cloud droplets. This approach illustrates an important difference from the work of Jacobson et al. (1994), in which all coagulated particles were combined into a single population, without respect to their initial source population.

The definition of the relationship between mass and number for section i and section $i + 1$ must be satisfied at each time step,

$$N_{\mathrm{p}_{ik}}(t) = \frac{\sum_{j,j\neq \mathrm{H_2O}} M_{\mathrm{p}_{ijk}}(t)}{\frac{\pi}{6}\rho_{\mathrm{p}_{ik}}(t)(D_{\mathrm{p}_i}^{\mathrm{dry}})^3} \tag{5}$$

$$N_{\mathrm{p}_{(i+1)k}}(t) = \frac{\sum_{j,j\neq \mathrm{H_2O}} M_{\mathrm{p}_{(i+1)jk}}(t)}{\frac{\pi}{6}\rho_{\mathrm{p}_{(i+1)k}}(t)(D_{\mathrm{p}_{i+1}}^{\mathrm{dry}})^3}, \tag{6}$$

where $D_{\mathrm{p}_i}^{\mathrm{dry}}$ is the mass mean diameter of dry components of section i and is fixed during the simulation such that

$$\frac{D_{\mathrm{p}_{(i+1)}}^{\mathrm{dry}}}{D_{\mathrm{p}_i}^{\mathrm{dry}}} = \text{constant}. \tag{7}$$

Conservation of mass,

$$M_{\mathrm{p}_{ijk}}(t) + M_{\mathrm{p}_{(i+1)jk}}(t) + \Delta t\left(\frac{\partial M_{\mathrm{p}_{ijk}}(t)}{\partial t} + \frac{\partial M_{\mathrm{p}_{(i+1)jk}}(t)}{\partial t}\right) = M_{\mathrm{p}_{ijk}}(t + \Delta t) + M_{\mathrm{p}_{(i+1)jk}}(t + \Delta t), \tag{8}$$

and conservation of particle number,

$$N_{\mathrm{p}_{ik}}(t) + N_{\mathrm{p}_{(i+1)k}}(t) + \Delta t\left(\frac{\partial N_{\mathrm{p}_{ik}}(t)}{\partial t} + \frac{\partial N_{\mathrm{p}_{(i+1)k}}(t)}{\partial t}\right) = N_{\mathrm{p}_{ik}}(t + \Delta t) + N_{\mathrm{p}_{(i+1)k}}(t + \Delta t), \tag{9}$$

provide the physical constraints to calculate the changes in M and N resulting from condensational growth or evaporation. The number of particles grown in a time step is then given by

$$J_{ik}^{\mathrm{grow}} \equiv N_{\mathrm{p}_{ik}}(t + \Delta t) - N_{\mathrm{p}_{ik}}(t), \tag{10}$$

where it is noted that

$$J_{ik}^{\mathrm{grow}} \neq \sum_j \left(\frac{M_{\mathrm{p}_{ijk}}}{\sum_j M_{\mathrm{p}_{ijk}}} m_{ik}\right) J_{ijk}^{\mathrm{cond}}. \tag{11}$$

The numerical algorithm was designed in modules, each describing a chemical or microphysical process. For specific sets of measurements, all quantities may not be available, so the model is designed to be initialized from aircraft-based field observations. The resulting predictions for variables can be compared to quantities measurable by research aircraft collecting vertically distributed observations in a Lagrangian framework.

The aerosol model is 0-dimensional but is embedded in a one-dimensional thermodynamic model to allow control of temporal cycling or variation in temperature and pressure. The one-dimensional structure can be predicted with an adiabatic cloud model or other vertical circulation model. Alternatively, direct measurements from laboratory, aircraft, or balloon soundings can be used to specify temperature, pressure and humidity gradients.

Number Conservation in Particle Growth

Accurately tracking changes in particle size requires careful attention in numerical models of aerosol dynamics. For complex aerosol-size distributions of mixed composition, the sectional approach, however, has proven effective in representing both particle growth and interparticle coagulation. A problem inherent in the sectional approach is artificial diffusion of particles among adjacent size bins (Wexler and Seinfeld, 1990; Dhaniyala and Wexler, 1996). Accurate advection algorithms, such as Accurate Space Derivatives (Dabdub and Seinfeld, 1994) and the Bott method (Bott, 1989; Bott, 1992), can fail to conserve particle number by apportioning additional mass to a particle number in a fixed-size bin because they track only one moment of the particle distribution, the mass. Consequently, the methods lack sufficient information to calculate growth in a number-conserving way. Since the number distribution of particles determines the number of nuclei available for cloud droplet formation, conservation of particle number in calculation of growth and coagulation is an important feature in determining aerosol-cloud interactions. This aspect of numerical modeling is, for example, critical to understanding ship tracks, since the tracks are characterized by significant changes in number concentrations of interstitial aerosol particles and cloud droplets (Radke et al., 1989).

The approach taken here utilizes results of a recent comparison of zero and higher order methods for solving the condensation equation (Kostoglou and Karabelas, 1994), which suggests that the zero-order solution employing simultaneous number and mass constraints is of accuracy comparable to or exceeding that of advanced higher order methods. Our independently derived zero-order method is mathematically equivalent to the approach of Tzivion et al. (1987) and is the general form of the equations employed by Hounslow et al. (1988) and Litster et al. (1995).

The condensation rate of species, such as H_2SO_4, SO_2, organic species, and H_2O, to aerosol particles is described using the modified form of the Fuchs-Sutugin equation (Hegg et al., 1992; Kreidenweis et al., 1991). The condensation rate J_{ijk}^{cond} ($\text{cm}^{-3}\ \text{s}^{-1}$) to a particle of ambient diameter $D_{\text{p}_{ik}}^{\text{amb}}$ is given by

$$J_{ijk}^{\text{cond}} = 2\pi \mathcal{D}_j D_{\text{p}_{ik}}^{\text{amb}} F(\text{Kn}_{ik}) A(\text{Kn}_{ik}) (P_j^{\infty} - P_{ijk}^{\text{surf}}), \quad (12)$$

where $\mathcal{D}_j$ is the diffusivity of species j ($\text{cm}^2\ \text{s}^{-1}$), Kn_{ik} is the Knudsen number (that is, the ratio of the air mean free path to the particle radius), $\text{Kn}_{ik} = 2\lambda / D_{\text{p}_{ik}}^{\text{amb}}$, $F(\text{Kn}_{ik})$ is a coefficient correcting for free molecular effects,

$$F(\text{Kn}_{ik}) = \frac{1 + \text{Kn}_{ik}}{1 + 1.71\text{Kn}_{ik} + 1.33\text{Kn}_{ik}^2}, \quad (13)$$

and A is a coefficient correcting for the interfacial mass transport limitations described by the accommodation coefficient a_e,

$$A(\text{Kn}_{ik}) = \left(1 + 1.33\text{Kn}_{ik} F(\text{Kn}_{ik}) \left(\frac{1}{a_e} - 1\right)\right)^{-1}. \quad (14)$$

Independence of Subsaturated and Supersaturated Vapor Growth

Condensation of a vapor under supersaturated conditions is treated as a dynamic process, as described by Eq. (12). Here we will use water as the supersaturated condensate, but other vapors could also be substituted. As described in Eqs. (2) and (4), growth due to condensation of nonsupersaturated solutes (SO_2 and H_2SO_4) is then calculated using fixed sections, Eq. (8) and (9). However, since the summation used in the definition Eq. (5) does not include water, growth of particles by addition of water will not alter the fixed sectional size class (denoted i) or its dry diameter, $D_{\text{p}_i}^{\text{dry}}$. Instead water condensation will be calculated using a moving sectional approach (Warren and Seinfeld, 1985b). Jacobson and Turco (1995) pro-

posed a similar approach but used a different algorithm for fixed sectional growth. The ambient diameter of particles and droplets ($D_{p_{ik}}^{amb}$) is described by

$$D_{p_{ik}}^{amb}(t) = \left(\frac{\sum_j M_{p_{ijk}}(t)}{\frac{\pi}{6} \rho_{p_{ik}}(t) N_{p_{ik}}(t)} \right)^{1/3} \quad (15)$$

for section i of population k. Note then that combining Eqs. (15) and (5) the difference between dry diameter ($D_{p_i}^{dry}$) and ambient diameter ($D_{p_{ik}}^{amb}(t)$) is determined from the mass of water per particle,

$$(D_{p_{ik}}^{amb}(t) - D_{p_i}^{dry}) = \left(\frac{M_{p_{i(H_2O)k}}(t)}{\frac{\pi}{6} \rho_{H_2O}(t) N_{p_{ik}}(t)} \right)^{1/3}. \quad (16)$$

The advantage of the moving sectional approach over fixed sections is that it avoids the loss of particle-size information that occurs when several classes of aerosol size are activated to nearly identical droplet sizes and particles of varying dry sizes are lumped into a single activated size class. This feature is also necessary to treat condensates that evaporate under atmospheric conditions (i.e., water), since evaporation to subsaturated conditions requires the information that is lost in lumping of size classes.

APPLICATION TO AN ATMOSPHERIC AEROSOL EVOLUTION STUDY

To illustrate the predictions of the model, we consider a case study from measurements taken during the Monterey Area Ship Tracks experiment off the coast of California in 1994. The measurements for this case indicate clean marine conditions under warm stratus conditions with a shallow temperature inversion at 600 m. The model described here also has been applied to a series of clean and polluted marine conditions reported in a comparative study in preparation. The thermodynamic structure of the cloud layer, extending from 400 to 600 m, is illustrated in Fig. 2.

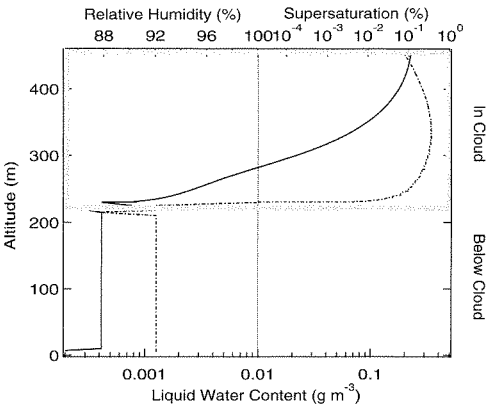

FIGURE 2. (a) The dotted line represents the supersaturation profile in cloud for rising and falling air parcels for the marine boundary layer sampled in June 1994. (b) The solid line illustrates the relationship of dry and ambient diameters during the activation and evaporation processes.

Lagrangian Air Parcel Dynamics

To characterize aerosol evolution in the boundary layer with a 0-D model over a period of hours to days, we consider a parcel of air moving at a variable wind speed in the direction of the mean wind. Wind speed and direction are measured from the aircraft. The parcel circulates within the boundary layer as a consequence of turbulence and is assumed to mix to the level of the temperature inversion measured in aircraft soundings. The rate of mixing is estimated from the vertical velocity. The air parcel is tracked through the use of a surrogate, such as a constant-altitude tracking balloon, a tracer release, or a ship track. The surrogate allows collection of measurements of the air parcel downwind of the initialization measurement for comparison to the model predictions.

Circulation in the boundary layer and through clouds is tracked through variations in pressure, temperature, and relative humidity. Clouds form when warm moist air from the surface rises so that the parcel is sufficiently cooled to result in supersaturation. The rate of parcel rise is described here from temperature profiles measured by aircraft or balloon soundings, so that the parcel

dynamics are controlled directly by observations.

Particle Sources and Sinks

Particle and vapor phase sources are described by parameterizations from field measurements. Vapor-particulate equilibria are calculated using the empirical correlation method of Pitzer (Pytkowicz, 1979), and chemical reactions of sulfates are estimated from field measurements (for example, Quinn et al., 1990). The primary flux in this case is sea salt, such that

$$J_{ik}^{\text{flux}} \equiv J_{ik}^{\text{salt}}. \tag{17}$$

Sea salt production of particles, J_{ik}^{salt} (cm^{-3} s^{-1}), is based on recent observations of steady state sea salt CCN number concentrations observed by Bigg et al. (1995), employing the size distribution shape measured in the laboratory work of Bowyer et al. (1990). Bigg et al. (1995) reported steady-state number concentrations of sea salt CCN in clean marine conditions that increased with wind speed. Using their measurements and assuming all other sources ($(\partial N_{\text{p}_{ijk}}(t)/\partial t)^{\text{nucl}}$, $(\partial N_{\text{p}_{ijk}}(t)/\partial t)^{\text{cond}}$, and $(\partial N_{\text{p}_{ijk}}(t)/\partial t)^{\text{coag}}$) to be negligible for their study, we can infer a rate of production of CCN from the steady state relationship

$$\frac{\partial N_{\text{p}_{ijk}}(t)}{\partial t} = \left(\frac{\partial N_{\text{p}_{ijk}}(t)}{\partial t}\right)^{\text{salt}} + \left(\frac{\partial N_{\text{p}_{ijk}}(t)}{\partial t}\right)^{\text{depn}} = 0, \tag{18}$$

such that

$$\left(\frac{\partial N_{\text{p}_{ijk}}(t)}{\partial t}\right)^{\text{salt}} = J_{ik}^{\text{salt}} = K_{ik}^{\text{depn}} 10^{0.48+0.043U}, \tag{19}$$

where U (m s^{-1}) is the wind speed and K_{ik} is the deposition constant in s^{-1}.

Formation of new particles is assumed to occur via the binary homogeneous nucleation of H_2SO_4 and H_2O. The rate of formation is calculated using classical binary nucleation theory including effects of hydrated sulfuric acid molecules (Laaksonen and Kulmala, 1991).

Formation of SO_2 and H_2SO_4 from dimethyl sulfide (DMS) is calculated using the rate expressions of DeMore et al. (1994) and the yield recommended in previous work (Pandis et al., 1994; Russell et al., 1994). Ambient hydroxyl radical concentrations that are required for oxidation of SO_2 to H_2SO_4 are calculated from available measurements of incident ultraviolet light, NO, NO_2, O_3, CO, HCHO, and other reactive organics using an atmospheric chemical reaction mechanism (Carter, 1990). A daytime average OH concentration is calculated and corrected for partial cloud cover conditions.

Particle Activation in Cloud

The water content of particles under subsaturated conditions can be assumed to be in local equilibrium with the ambient environment. This assumption is equivalent to

$$P_{i(\text{H}_2\text{O})k}^{\text{surf}} = P_{\text{H}_2\text{O}}^{\infty}. \tag{20}$$

The time required to reach this equilibrium is a function of humidity, temperature, solute activity, and number concentration. For typical ambient subsaturated conditions that time is approximately 0.1 s (Pandis et al., 1995), making the assumption of equilibrium appropriate when ambient humidity is changing on a time scale longer than this characteristic time. Since the integral method used is zero order, the algorithm can become unstable under haze conditions (90% to 99% relative humidity) using time steps of 1 s or longer if this assumption is not employed.

Under supersaturated conditions the time required to reach water equilibrium can be significantly longer than that under subsaturated conditions. In warm stratus layers with low updraft velocities and weak supersaturations, the rate of change of the supersaturation can be comparable to or faster than the rate of particle growth. This condition implies that activation of particles will not occur as an equilibrium process so that Eq. (20) is not used. For relative humidities greater than 100%, water conden-

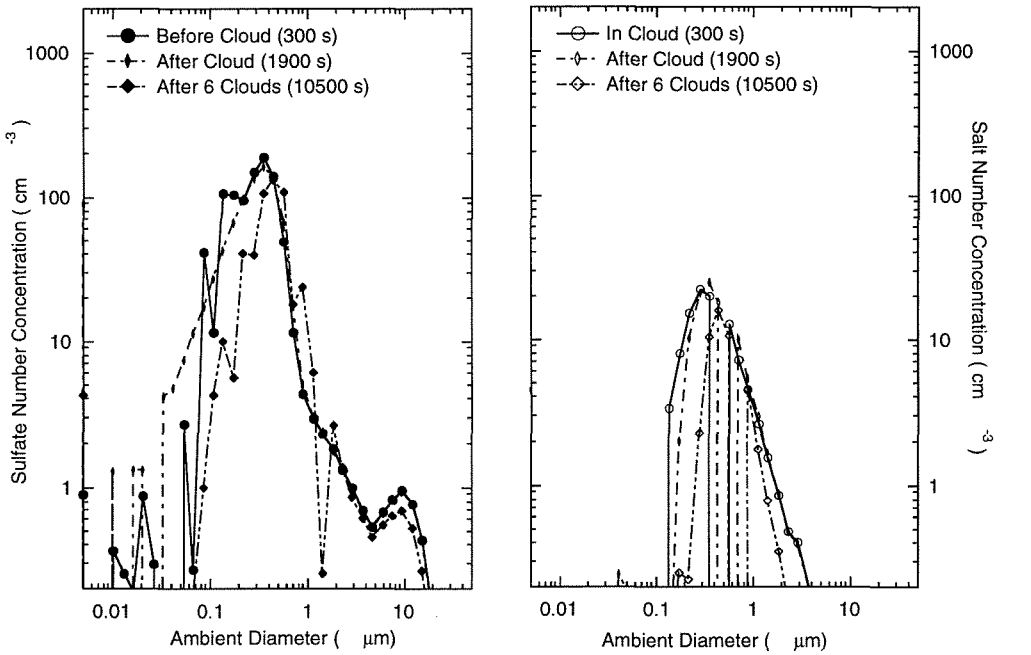

FIGURE 3. The left graph represents the sulfate aerosol population number concentration below cloud, and the right graph shows the same for the salt aerosol number population concentration. The curves illustrate the population before processing by a cloud after 300 s of simulation, after processing by a cloud at 1900 s of simulation, and after processing by six cloud cycles at 10,500 s of simulation.

sation is calculated from Eq. (12) with $j = H_2O$.

This approach contrasts with previous works (Ackerman et al., 1995; Pandis et al., 1995; Flossman et al., 1985) who have employed the equilibrium relation for droplet activation (Pruppacher and Klett, 1978) to calculate cloud droplet number concentrations for prescribed supersaturations. The accuracy of this assumption has not been investigated for the formation of clouds in anthropogenically dominated aerosol conditions. This model incorporates the full dynamic calculation in order to address such questions.

Water activities are calculated using the Pitzer method (Pytkowicz, 1979; Zemaitis, 1986). Chemical equilibrium in aqueous solution is described based on field observations (Quinn et al., 1990).

Predictions for Clean Aerosol Evolution in a Stratus-Capped Marine Boundary Layer

In this case study, the ratio of ammonium sulfate to ammonium bisulfate is set to 1, based on measurements of ionic composition of particles in the Pacific marine boundary layer (Quinn et al., 1990). Near the California coast anthropogenic influences are estimated to be sufficiently strong that H_2O_2 and other oxidants are in excess for droplet and particle aqueous oxidation, namely

$$P^{\text{surf}}_{i(SO_2)k} = 0. \tag{21}$$

The initial size distribution is indicated in Fig. 3. Figure 3 also shows the effect of cloud processing by both a single cloud cycle and by multiple (six) cloud cycles on particle number concentration and size. The results clearly show growth of particles of both types

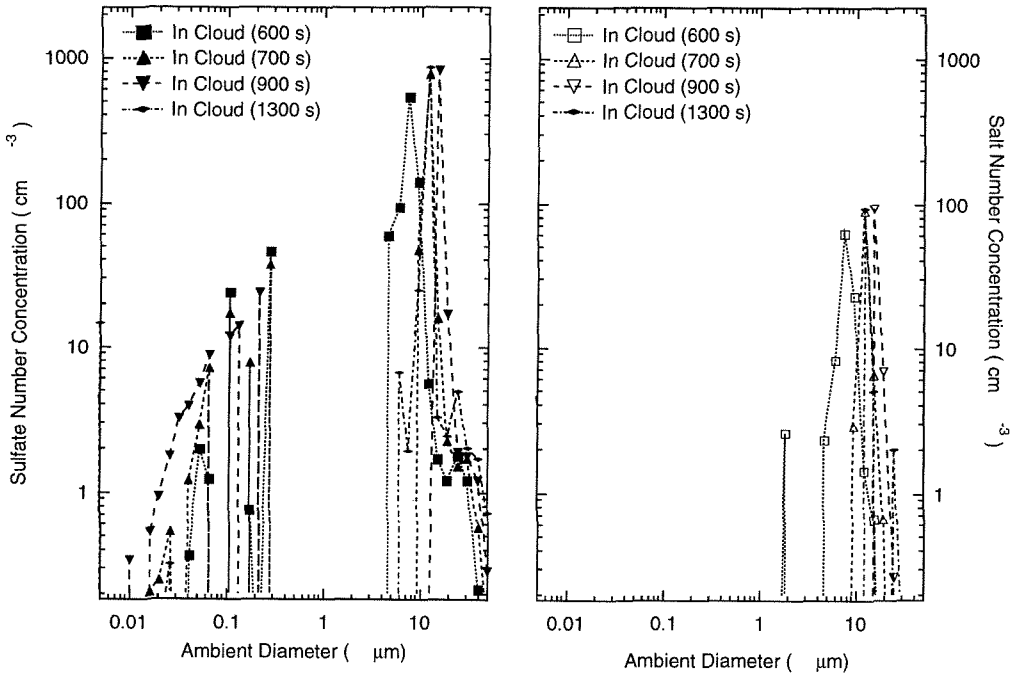

FIGURE 4. The left graph represents the sulfate aerosol population number concentration in cloud with changing supersaturation, and the right graph shows the same for the salt aerosol number population concentration. The curves illustrate the population during the growth-rate limited activation process in the first cloud cycle at simulation times of 600 s, 700 s, 900 s, and 1300 s.

("sulfate"-type aerosol and "salt"-type aerosol). For the salt particles there is an increase in the size of the peak modal concentration after cloud processing, whereas for the sulfate particles the particle growth is significant but less distinct.

Figure 4 illustrates the changes in the particle-size distribution during the activation of the particles in the cloud. As the supersaturation initially increases, smaller particles are activated and the predicted cloud droplet size increases. More detailed simulations of this type investigate the role of aerosol particle concentration on determining the droplet distribution using data from the Monterey Area Ship Track Experiment.

The model also predicts the change in the internal mixture for each size class of each population. Figures 5 and 6 illustrate the change in composition due to cloud processing. For both the sulfate aerosol and the salt aerosol, the mass fraction of sulfate and bisulfate increase during cloud processing for particles in dry diameter sections between 0.2 and 0.8 μm.

For the conditions investigated here, namely a stratus-capped marine boundary layer with very low anthropogenic sulfur dioxide concentrations and a DMS flux of 5 μmole m^{-2} d^{-1}, no homogeneous nucleation of hydrated sulfuric acid was predicted. Since the stratus layer consisted of almost half of the height of the boundary layer, the air parcel spent close to half of the time in cloud. This processing removed much of the condensable sulfuric acid and precursors that otherwise might have nucleated.

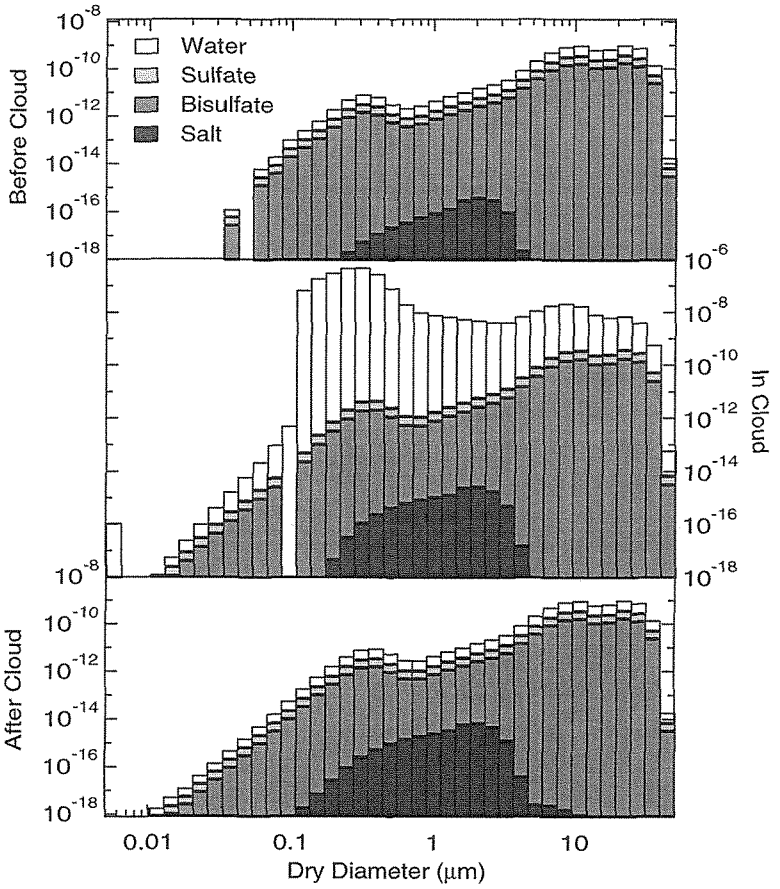

FIGURE 5. The bar graphs represent the mass of each component $\left(\frac{dMp_{ijk}}{d \log D_{p_i}^{\text{dry}}} \text{ in gcm}^{-3}\right)$ **of the aerosol distribution for the sulfate aerosol population, where the abscissa of dry diameter uses the sectional diameter that excludes water. Ammonium sulfate and bisulfate are shaded gray, and sodium chloride is filled with dots.**

CONCLUSIONS

Model Development

The work described here presents a new model for calculating the evolution of externally mixed populations of internally mixed aerosol particles. The algorithm describes the processes of nucleation, condensation, coagulation and deposition. The model combines a fixed-section representation for coagulation and growth of subsaturated species and a moving-section representation of growth and evaporation of supersaturated species. And, the dual moment sectional approach to growth conserves particle number and mass.

Application to Cloud-Aerosol Interaction

Both natural and anthropogenic aerosol in the atmosphere are controlled by vapor-particle mass transfer and interparticle coagulation. Cloud formation and processing changes the dynamics of the particle population by increasing the particulate surface area and the collision cross section. To understand these processes, we have applied this numerical model and initialized it with data measured in the atmosphere. We have investigated the role of aerosols from several marine boundary layer sources, including sea spray and biogenic sulfur, and have an-

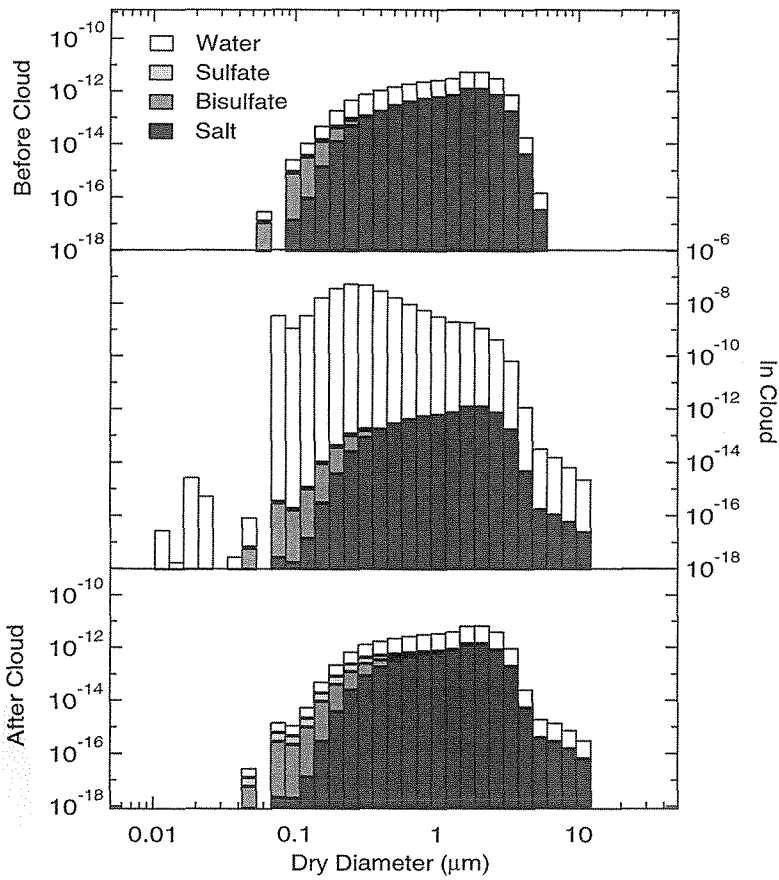

FIGURE 6. The bar graphs represent the mass of each component $\left(\frac{dMp_{ijk}}{d \log D_{p_i}^{\text{dry}}} \text{ in g cm}^{-3}\right)$ **of the aerosol distribution for the salt aerosol population, where the abscissa of dry diameter uses the sectional diameter, which excludes water. Ammonium sulfate and bisulfate are shaded gray, and sodium chloride is filled with dots.**

alyzed the differential growth patterns in each aerosol population for cloud processing and subcloud sulfate condensation. Sulfate-type and salt-type particle populations include internal mixtures of solutes for each size class.

LMR is indebted to the National Science Foundation Advanced Study Program at the National Center for Atmospheric Research for providing support for the development of this model. The authors also thank the Office of Naval Research for providing support for field research that demonstrated the need for the work reported here.

References

Ackerman, A. S., Toon, O. B., and Hobbs, P. V. (1995). A Model for Particle Microphysics, Turbulent Mixing, and Radiative Transfer in the Stratocumulus-Topped Marine Boundary Layer and Comparisons with Measurements, *J. Atmos. Sci.* 52:1204.

Bigg, E. K., Gras, J. L., and Mossop, D. J. C. (1995). Wind-Produced Submicron Particles in the Marine Atmosphere, *Atmos. Res.* 36:55–68.

Bott, A. (1989). A Positive Definite Advection Scheme Obtained by Nonlinear Renormalization of the Advective Fluxes, *Mon. Wea. Rev.* 117:1006–1015.

Bott, A. (1992). Monotone Flux Limitation in the Area-Preserving Flux-Form Advection Algorithm, *Mon. Wea. Rev.* 120:2592–2602.

Bowyer, P. A., Woolf, D. K., and Monahan, E. C. (1990). Temperature Dependence of the Charge and Aerosol Production Associated with a Breaking Wave in a Whitecap Simulation Tank, *J. Geophys. Res.* 95:5313–5319.

Carter, W. P. L. (1990). A Detailed Mechanism

for the Gas-Phase Atmospheric Reactions of Organic-Compounds, *Atmos. Environment* 24A, 481–518.

Charlson, R. J., Lovelock, J. E., Andreae, M. O., and Warren, S. G. (1987). Oceanic Phytoplankton, Atmospheric Sulfur, Cloud Albedo and Climate, *Nature* 326:665–661.

Dabdub, D., and Seinfeld, J. H. (1994). Numerical Advective Schemes Used in Air-Quality Models—Sequential and Parallel Implementation, *Atmos. Environment* 28:3369–3385.

DeMore, W. B., Sander, S. P., Golden, D. M., Hampson, R. F., Kurylo, M. J., Howard, C. J., Ravishankara, A. R., Kolb, C. E., and Molina, M. J. (1994). *Chemical Kinetics and Photochemical Data for Use in Stratospheric Modeling*, Evaluation Number 11, NASA-JPL Publication 94-26.

Dhaniyala, S., and Wexler, A. S. (1996). Numerical Schemes to Model Condensation and Evaporation of Aerosols, *Atmos. Environment* 30:919–928.

Flossmann, A. I., Hall, W. D., and Pruppacher, H. R. (1985). A Theoretical Study of the Wet Removal of Atmospheric Particles Captured through Nucleation and Impaction Scavenging by Growing Cloud Drops, *J. Atmos. Sci.* 42: 583–606.

Hallett, J., Hudson, J. G., and Rogers, C. F. (1989). Characterization of Combustion Aerosols for Haze and Cloud Formation, *Aerosol Sci. Tech.* 10:70–83.

Haywood, J. M., and Shine, K. D. (1995). The Effect of Anthropogenic Sulfate and Soot Aerosol on the Clear Sky Radiation Budget, *Geophys. Res. Lett.* 22:603–606.

Hegg, D. A., Radke, L. F., and Hobbs, P. V. (1990). Particle Production Associated with Marine Clouds, *J. Geophys. Res.* 95:13917–13926.

Hegg, D. A., Covert, D. S., and Kapustin, C. F. (1992). Modeling a Case of Particle Nucleation in the Marine Boundary-Layer, *J. Geophys. Res.* 97:9851–9857.

Hounslow, M. J., Ryall, R. L., and Marshall, V. R. (1988). A Discretized Population Balance for Nucleation, Growth, and Aggregation, *AIChE Journal*, 34:1821–1832.

Jacobson, M. Z., and Turco, R. P. (1995). Simulating Condensational Growth, Evaporation, and Coagulation of Aerosols Using a Combined Moving and Stationary Size Grid, *Aerosol Sci. Tech.* 22:73–92.

Jacobson, M. Z., Turco, R. P., Jensen, E. J., and Toon, O. B. (1994). Modeling Coagulation among Particles of Different Composition and Size, *Atmos. Environ.* 28:1327–1338.

Kostoglou, M., and Karabelas, A. J. (1994). Evaluation of Zero-Order Methods for Simulating Particle Coagulation, *J. Coll. I. Sci.* 163:420–431.

Kreidenweis, S. M., Penner, J. E., Yin, F., and Seinfeld, J. H. (1991). The Effects of Dimethylsulfide upon Marine Aerosol Concentrations, *Atmos. Env.* 25:2501–2511.

Laaksonen, A., and Kulmala, M. (1991). Homogeneous Heteromolecular Nucleation of Sulfuric-Acid and Water Vapors in Stratospheric Conditions—A Theoretical-Study of the Effect of Hydrate Interaction, *J. Aerosol Sci.* 22:779–787.

Liao, H., and Seinfeld, J. H. (1998). Effects of Clouds and Direct Radiative Forcing of Climate, *J. Geophys. Res.* in press.

Litster, J. D., Smit, D. J., and Hounslow, M. J. (1995). Adjustable Discretized Population Balance for Growth and Aggregation, *AIChE Journal* 41:591–603.

National Research Council (1996). *A Plan for a Research Program on Aerosol Radiative Forcing and Climate Change*, National Academy Press, Washington, D.C.

Pandis, S. N., Russell, L. M., and Seinfeld, J. H. (1994). The Relationship between DMS Flux and CCN Concentration in Remote Marine Regions, *J. Geophys. Res.* 99:16,945–16,957.

Pandis, S. N., Wexler, A. S., and Seinfeld, A. S. (1995). Dynamics of Tropospheric Aerosols, *J. Phys. Chem.* 99:9646.

Pruppacher, H. R., and Klett, J. D. (1978). *Microphysics of Clouds and Precipitation*, Reidel Publishing, Dordrecht, Netherlands.

Pytkowicz, R. M. (ed.) (1979). *Activity Coefficients in Electrolyte Solutions*, CRC Press, Boca Raton, FL.

Quinn, P. K., Bates, T. S., Johnson, J. E., Covert, D. S., and Charlson, R. J. (1990). Interactions between the Sulfur and Reduced Nitrogen Cycles over the Central Pacific Ocean, *J. Geophys. Res.* 95:16,405.

Radke, L. F., Coakley, J. A., and King, M. D. (1989). Direct and Remote-Sensing Observa-

tions of the Effects of Ships on Clouds, *Science* 246:1146.

Russell, L. M., Pandis, S. N., and Seinfeld, J. H. (1994). Aerosol Production and Growth in the Marine Boundary Layer, *J. Geophys. Res.* 99: 20,989–21,003.

Tzivion, S., Feingold, G., and Levin, Z. (1987). An Efficient Numerical Solution to the Stochastic Collection Equation, *J. Atmos. Sci.* 44: 3139–3149.

Warren, D., and Seinfeld, J. H. (1985a). Prediction of Aerosol Concentrations Resulting from a Burst of Nucleation, *J. Colloid Interface Sci.* 105:136–142.

Warren, D., and Seinfeld, J. H. (1985b). Simulation of Aerosol Size Distribution Evolution in Systems with Simultaneous Nucleation, Condensation and Coagulation, *Aerosol Sci. Tech.* 4:31–43.

Wexler, A. S., and Seinfeld, J. H. (1990). The Distribution of Ammonium Salts Among a Size and Composition Dispersed Aerosol, *Atmos. Env.* 24:1231–1246.

Wexler, A. S., and Seinfeld, J. H. (1992). Analysis of Aerosol Ammonium-Nitrate—Departures from Equilibrium during SCAQS, *Atmos. Environment* 26A:579–591.

Zemaitis, J. F. (ed.) (1986). *Handbook of Aqueous Electrolyte Thermodynamics*, McGraw-Hill, New York.

Received June 13, 1997; accepted November 10, 1997.